JACS
JOURNAL OF THE AMERICAN CHEMICAL SOCIETY

COMMUNICATION

pubs.acs.org/JACS

Dependence of Single-Molecule Conductance on Molecule Junction Symmetry

Masateru Taniguchi,*[,†] Makusu Tsutsui,[†] Ryoji Mogi,[‡] Tadashi Sugawara,[‡] Yuta Tsuji,[§] Kazunari Yoshizawa,[§] and Tomoji Kawai*[,†]

[†]The Institute of Scientific and Industrial Research, Osaka University, Ibaraki, Osaka 567-0047, Japan

[‡]Department of Basic Science, Graduate School of Arts and Sciences, The University of Tokyo, 3-8-1 Komaba, Meguro-ku, Tokyo 153-8902, Japan

[§]Institute for Materials Chemistry and Engineering, Kyushu University, 744 Motooka, Nishi-ku, Fukuoka 819-0395, Japan

Supporting Information

ABSTRACT: The symmetry of a molecule junction has been shown to play a significant role in determining the conductance of the molecule, but the details of how conductance changes with symmetry have heretofore been unknown. Herein, we investigate a naphthalenedithiol single-molecule system in which sulfur atoms from the molecule are anchored to two facing gold electrodes. In the studied system, the highest single-molecule conductance, for a molecule junction of 1,4-symmetry, is 110 times larger than the lowest single-molecule conductance, for a molecule junction of 2,7-symmetry. We demonstrate clearly that the measured dependence of molecule junction symmetry for single-molecule junctions agrees with theoretical predictions.

Recent dramatic progress in creating single-molecule devices has led to fabrication of semiconductor-related products such as field-effect transistors,[1] diodes,[2] electroluminescence devices,[3] and even emerging nanodevices that use molecular motion as a switching parameter.[4,5] The key issue that determines how single-molecule devices operate and how their characteristics can be controlled is the symmetry of an electrode−molecule junction where two atoms from the molecule are anchored to two facing electrodes.[6−15] A comprehensive understanding of how single-molecule conductance changes with molecule junction symmetry would facilitate the design and synthesis of functional molecules for single-molecular devices.

We previously developed the orbital symmetry rule for electron transport in single-molecule junctions. When we applied the rule to single-molecule junctions of four naphthalenedithiol (ND) isomers,[16,17] the rule correctly predicted whether frontier molecular orbitals on atoms anchored to two facing gold electrodes should exhibit large or small single-molecule conductance. We have carried out the present study to validate our previous theoretical predictions.

Our orbital symmetry rule specifies that when the Fermi level (E_F) of the electrodes is between the energies of the highest occupied molecular orbital (ε_{HOMO}) and the lowest unoccupied molecular orbital (ε_{LUMO}), the transmission probability is qualitatively predicted from the contribution of the HOMO and LUMO in the isolated molecular Green's function (eq 1).

$$\frac{C_{R,HOMO}C^*_{L,HOMO}}{E_F - \varepsilon_{HOMO}} + \frac{C_{R,LUMO}C^*_{L,LUMO}}{E_F - \varepsilon_{LUMO}} \quad (1)$$

where $C_{R,HOMO}$ and $C_{R,LUMO}$ are the molecular-orbital expansion coefficient at a sulfur atom connected to the right electrode at the HOMO and LUMO, respectively, and the other terms are comparably assigned (see Supporting Information).

This equation implies that when the signs of the two products $C_{R,HOMO}C^*_{L,HOMO}$ and $C_{R,LUMO}C^*_{L,LUMO}$ differ, Au−single-molecule−Au junctions are symmetry allowed and exhibit high single-molecule conductance; when the signs of the two products are the same, the junctions are symmetry forbidden and exhibit low single-molecule conductance. For the case of two degenerate states where the HOMO and LUMO in eq 1 are replaced by singly occupied molecular orbital 1 (SOMO1) and SOMO2, the opposite orbital symmetry rule applies: when the signs of the two products $C_{R,SOMO1}C^*_{L,SOMO1}$ and $C_{R,SOMO2}C^*_{L,SOMO2}$ differ, the junctions are symmetry forbidden. Consequently, the dependence of single-molecule conductance on junction symmetry can be predicted only by the phases of the sulfur atoms on the frontier molecular orbitals.

To investigate our orbital symmetry rule for electron transport, we selected ND as a small thiol molecule. We examined the conductance of single-molecule junctions of 2,6-ND, 2,7-ND, 1,4-ND, and 1,5-ND (Figure 1), which we synthesized successfully (Figures S1 and S2).

We calculated transmission probabilities at the Hückel level of theory for the four ND-isomer junctions. Figure 2 shows the calculated electron transmission spectra. Resonance peaks for 2,6-ND, 1,5-ND, and 1,4-ND appear at the Fermi level, indicating that frontier molecular orbitals interfere constructively, and an antiresonance peak for 2,7-ND appear at the Fermi level, indicating that frontier molecular orbitals interfere destructively. This orbital symmetry rule for electron transport agrees well with the quantum interference discussion.[18−21] Consequently, the single-molecule conductance order becomes 2,7-ND (0 G_0, where G_0 is the conductance quantum, 77.5 μS) < 2,6-ND (0.82 G_0) and 1,5-ND (0.82 G_0) < 1,4-ND (0.94 G_0) at the Fermi level.

Received: April 13, 2011
Published: July 08, 2011

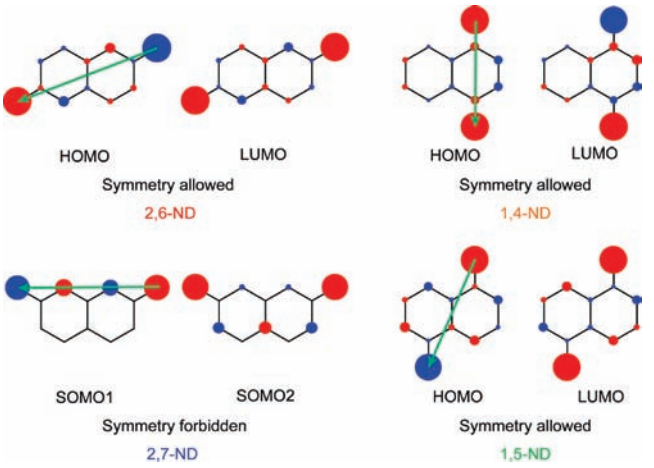

Figure 1. Frontier molecular orbitals (HOMO, LUMO, and SOMO) of the four studied ND isomers at the Hückel molecular orbital theory level. SOMO1 and SOMO2 orbitals are degenerate. The phase and amplitude of these frontier orbitals determine that the route for electron transmission is symmetry forbidden for 2,7-ND and symmetry allowed for the other three isomers. Blue and red isosurfaces represent positive and negative isovalues, respectively; green arrows show the routes for electron transmission.

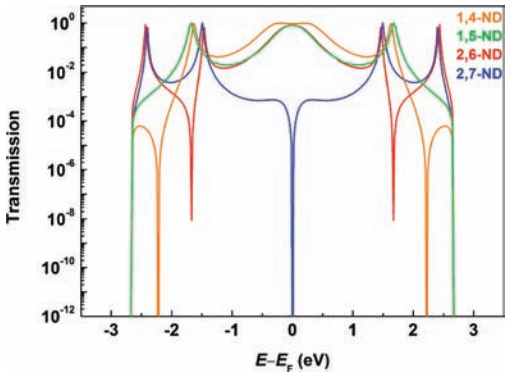

Figure 2. Calculated electron transmission spectra of Au−ND−Au single-molecule junctions at the Hückel level of theory. Calculated single-molecule conductances for the ND isomers are as follows: 1, 4-ND, 0.94 G_0; 1,5-ND, 0.82 G_0; 2,6-ND, 0.82 G_0; and 2,7-ND, 0 G_0, where G_0 is the conductance quantum, 77.5 μS. E_F is the Fermi energy of the electrodes.

The single-molecule conductance order is retained in the small bias window from −1 to +1 V.

We measured single-molecule conductances for the four ND-isomer junctions (0.2 V, room temperature, in vacuum) using nanofabricated mechanically controllable break junctions (Figure S3).[22,23] Figure 3 shows the measured conductance characteristics. Conductance traces obtained during the breaking process show three conductance plateaus—at 1 G_0, ~1 mG_0, and <1 mG_0 (Figure 3a)—that correspond to the formation of a single-gold atomic contact and of single-molecule junctions of 2,6-ND and 2,7-ND, respectively. Traces of tetrahydrofuran (THF) solvent decrease exponentially with time, indicating direct tunneling between electrodes (Figure S4). Conductance histograms show pronounced conductance peaks at ~1.4 and 0.1 mG_0 (Figures 3c and 3d). For 2,6-ND and 2,7-ND, single-molecule

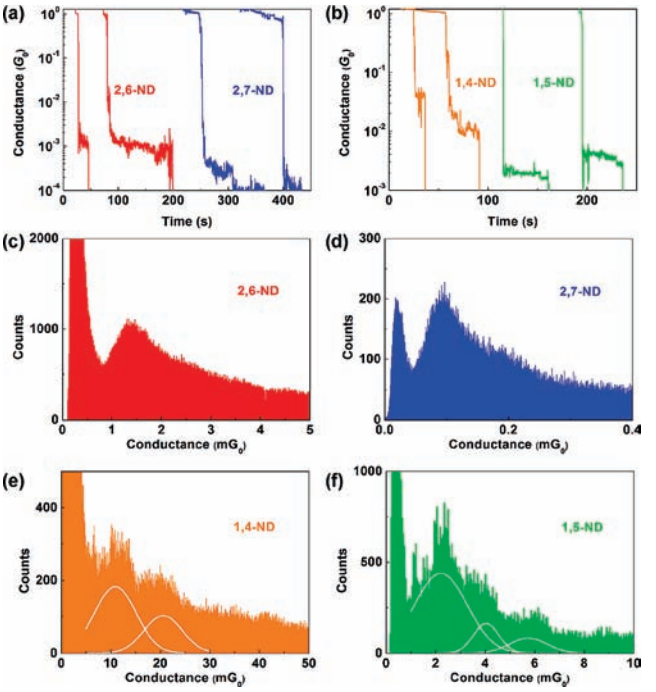

Figure 3. Measured conductance characteristics of Au−ND−Au single-molecule junctions: Typical conductance traces of (a) 2,6-ND and 2,7-ND and (b) 1,4-ND and 1,5-ND junctions. Conductance histograms of (c) 2,6-ND, (d) 2,7-ND, (e) 1,4-ND, and (f) 1,5-ND junctions constructed from 328, 365, 443, and 142 conductance traces, respectively (Figures S5 and S6). One thousand conductance traces were accumulated for all molecular junctions. Measured single-molecule conductances for the ND isomers are as follows: 2,6-ND, 1.4 mG_0; 2,7-ND, 0.1 mG_0; 1,4-ND, 11 mG_0; and 1,5-ND, 2.2 mG_0. Peak conductances for 1,4-ND and 1,5-ND were obtained at integral multiples of 11 and 2.2 mG_0, respectively. White lines are Gaussian fits to the peak profiles. All electrical measurements were performed at room temperature in a vacuum of 10^{-5} Torr.

conductances are 1.4 and 0.1 mG_0, respectively. For 1,4-ND and 1,5-ND, plateaus appear at ~10 mG_0 and several mG_0, respectively, and pronounced peaks appear at integral multiples of 11 and 2.2 mG_0 (Figure 3e,f). Thus, the measured single-molecule conductances of 1,4-ND and 1,5-ND are 11 and 2.2 mG_0, respectively, and the single-molecule conductance order is 2, 7-DN (0.1 mG_0) < 2,6-DN (1.4 mG_0) < 1,5-DN (2.2 mG_0) < 1, 4-DN (11 mG_0), where the highest conductance is 110 times the lowest.

We explored the voltage dependence of single-molecule conductance by measuring current−voltage characteristics at bias voltages of −0.8 to 0.8 V when the nanoelectrode gaps were fixed in the state where single-molecule conductance was obtained (Figure 4a). In the voltage window, the current−voltage characteristics show single-molecule conductance in the order 1,4-ND > 1,5-ND > 2,6-ND > 2,7-ND.

We found a remarkable result that neither the theoretical nor experimental conductance followed the exponential decay law (Figure 4b), although the exponential decrease in single-molecule conductance with increasing distance between sulfur atoms indicated electron tunneling.[24,25] Exponential-distance scaling is known to fail for either of the two scenarios:[26,27] (1) when electrode−molecule coupling energy is strong compared to half of the HOMO−LUMO gap or (2) when site−site interaction in

dx.doi.org/10.1021/ja2033926 |J. Am. Chem. Soc. 2011, 133, 11426–11429

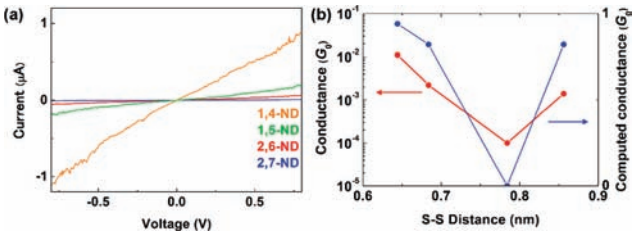

Figure 4. Measured electron-transport characteristics through Au−ND−Au single-molecule junctions for the four studied ND isomers. (a) Current−voltage characteristics of the four ND single-molecule junctions. (b) Single-molecule conductance as a function of distance between S atoms. The distances were obtained from optimized molecular structures, where the calculated S−S distances are as follows: 1,4-DN, 0.644 nm; 1,5-DN, 0.684 nm; 2,7-DN, 0.784 nm; and 2,6-DN, 0.856 nm. The dependence of single-molecule conductance on S−S distance obtained from experiments is similar to that obtained from theoretical calculations, and both disobey the exponential decay law with respect to distance.

the molecule is sufficiently strong to drive the single-molecule junction close to resonance tunneling. Our density functional theory (DFT) calculations yield the following HOMO−LUMO gaps: 2,6-ND, 4.3 eV; 2,7-ND, 4.5 eV; 1,4-ND, 4.1 eV; and 1,5-ND, 4.3 eV. However, theoretical calculations also yield electrode−molecule coupling energies of <1 eV;[28,29] hence, the first scenario is not applicable to ND junctions. However, the second scenario is applicable because for 2,6-ND, 1,4-ND, and 1,5-ND, π electrons on carbon and sulfur atoms interact strongly with each other at the frontier molecular orbitals (Figure 1). In addition, the theoretical and experimental conductance values differ. Theoretical calculations predict that, if the sole mechanism of electron transport is π tunneling, single-molecule conductance for 2,7-ND should become 0 at the Fermi level and for 1,4-ND, 1,5-ND, and 2,6-ND, single-molecule conductance should become close to 1 G_0. We carried out molecular projected self-consistent Hamiltonian (MPSH) analysis at the DFT level, which shows us the spatial distribution of the orbital levels modified by the electrodes. We performed two types of analysis: one without including the gold atoms and the other including the first-layer gold atoms. The results are shown in the Supporting Information (Figure S7). The MPSH analysis for the molecule itself shows that the orbitals near the Fermi level are π type; thus, σ orbitals do not contribute to conduction, which rationalizes the π-tunneling mechanism. On the other hand, the MPSH analysis that included the first-layer gold atoms showed that the MPSH states closest to the Fermi level are composed of σ-type orbitals of Au−S bonds. Although the energy levels of naphthalene π-states are somewhat farther from the Fermi level than Au−S σ-states, the mechanism of electron transport near the Fermi level could be attributed to the hybridization of σ and π tunneling. Thus, experimental conductance values are smaller than the theoretical values for 2,6-ND, 1,4-ND, and 1,5-ND and residual conductance exists for 2,7-ND because of σ-bonding tunneling.[18−20]

In summary, we found that differences in the symmetry of ND single-molecule junctions correspond strongly to differences in the single-molecule conductance of the junctions. Although all of the studied ND isomers have similar energy gaps and molecular orbital levels, the highest and lowest single-molecule conductances differ by a factor of 110. This large difference originates not from the difference in energy gaps and molecular orbital levels but rather from the difference in the frontier molecular orbital phases of the two sulfur atoms anchored to the electrodes. Thus, we have demonstrated clearly that molecular orbital theory provides an orbital symmetry rule for describing electron transport in single-molecule junctions as well as in chemical reactions. Further, the rule holds true even if the effects of molecule−electrode coupling by sulfur atoms are included.[30] The orbital symmetry rule for electron transport in single-molecule junctions provides a guiding principle for the design of molecules that exhibit desirable levels of single-molecule conductance.

■ ASSOCIATED CONTENT

Supporting Information. Synthesis and single-molecule measurements of dithiolnaphthalene and theoretical calculations of electron transmission for single-molecule junctions. This material is available free of charge via the Internet at http://pubs.acs.org.

■ AUTHOR INFORMATION

Corresponding Author
taniguti@sanken.osaka-u.ac.jp; kawai@sanken.osaka-u.ac.jp

■ ACKNOWLEDGMENT

This research is partially supported by the Japan Society for the Promotion of Science (JSPS) through its Funding Program for World-Leading Innovative R&D on Science and Technology. K.Y. acknowledges Grants-in-Aid (No. 18GS0207 and 22245028) for Scientific Research from JSPS and MEXT, the Kyushu University Global COE Project, the Nanotechnology Support Project, the MEXT Project of Integrated Research on Chemical Synthesis, and CREST of the Japan Science and Technology Cooperation.

■ REFERENCES

(1) Song, H.; Kim, Y.; Jang, Y. H.; Jeong, H.; Reed, M. A.; Lee, T. *Nature* **2009**, *462*, 1039.
(2) Díez-Pérez, I.; Hihath, J.; Lee, Y.; Yu, L.; Adamska, L.; Kozhushner, M. A.; Oleynik, I. I; Tao, N. J. *Nat. Chem.* **2009**, *1*, 635.
(3) Marquardt, C. W.; Grunder, S.; Błaszczyk, A.; Dehm, S.; Hennrich, F.; v. Löhneysen, H.; Mayor, M.; Krupke, R. *Nat. Nanotechnol.* **2010**, *5*, 863.
(4) Quek, S. Y.; Kamenetska, M.; Steigerwald, M.; Choi, H. J.; Louie, S. G.; Hybertsen, M. S.; Neaton, J. B.; Venkataraman, L. *Nat. Nanotechnol.* **2009**, *4*, 230.
(5) Parks, J. J.; Champagne, A. R.; Costi, T. A.; Shum, W. W.; Pasupathy, A. N.; Neuscamman, E.; Flores-Torres, S.; Cornaglia, P. S.; Aligia, A. A.; Balseiro, C. A.; Chan, G. K. L.; Abruna, H. D.; Ralph, D. C. *Science* **2010**, *328*, 1370.
(6) Tao, N. J. *Nat. Nanotechnol.* **2006**, *1*, 173.
(7) Lindsay, S. M.; Ratner, M. A. *Adv. Mater.* **2007**, *19*, 23.
(8) Chen., F.; Li, X.; Hihath, J.; Huang, Z.; Tao, N. J. *J. Am. Chem. Soc.* **2006**, *128*, 15874.
(9) Li, X.; Hihath, J.; Chen., F.; Masuda, T.; Zang, L.; Tao, N. J. *J. Am. Chem. Soc.* **2007**, *129*, 11535.
(10) Quinn, J. R.; Foss, F. W.; Venkataramn, L.; Hybersen, M. S.; Breslow, R. *J. Am. Chem. Soc.* **2007**, *129*, 6714.
(11) Park, Y. S.; Whalley, A. C.; Kamenetska, M.; Steigerwald, M. L.; Hybertsen, M. S.; Nuckolls, C.; Venkataraman, L. *J. Am. Chem. Soc.* **2007** *129*, 15768.
(12) Martin, C. A.; Ding, D.; Sørensen, J. K.; Bjørnholm, T.; van Ruitenbeek, J. M.; van der Zant, H. S. J. *J. Am. Chem. Soc.* **2008**, *130*, 13198.

(13) Taniguchi, M.; Tsutsui, M.; Shoji, K.; Fujiwara, H.; Kawai, T. *J. Am. Chem. Soc.* **2009**, *131*, 14146.
(14) Park, Y. S.; Widawsky, J. R.; Kamenetska, M.; Steigerwald, M. L.; Hybertsen, M. S.; Nuckolls, C.; Venkataraman, L. *J. Am. Chem. Soc.* **2009**, *131*, 10820.
(15) Yokota, K.; Taniguchi, M.; Tsutsui, M.; Kawai, T. *J. Am. Chem. Soc.* **2010**, *132*, 17364.
(16) Tada, T; Yoshizawa, K *ChemPhysChem* **2002**, *3*, 1035.
(17) Yoshizawa, K.; Tada, T.; Staykov, A. *J. Am. Chem. Soc.* **2008**, *130*, 9406.
(18) Cardmone, D. M.; Stafford, C. A.; Mazumdar, S. *Nano Lett.* **2006**, *6*, 2422.
(19) Ke, S.−H.; Yang, W.; Baranger, H. U. *Nano Lett.* **2008**, *8*, 3257.
(20) Solomon, G. C.; Andrews, D. Q.; Hansen, T.; Goldsmith, R. H.; Wasielewski, M. R.; van Duyne, R. P.; Ratner, M. *J. Chem. Phys.* **2008**, *129*, 054701.
(21) Solomon, G. C.; Herrmann, C.; Hansen, T.; Mujica, V.; Ratner, M. A. *Nat. Chem.* **2010**, *2*, 223.
(22) van Ruitenbeek, J. M.; Alvarez, A.; Pineyro, I.; Grahmann, C.; Joyez, P.; Devoret, M. H.; Esteve, D.; Urbina, C. *Rev. Sci. Instrum.* **1996**, *67*, 108.
(23) Tsutsui, M.; Shoji, K.; Taniguchi, M.; Kawai, T. *Nano Lett.* **2008**, *8*, 345.
(24) Xu, B.; Tao, N. J. *Science* **2003**, *301*, 1221.
(25) Venkataraman, L.; Klare, J. E.; Nuckolls, C.; Hybertsen, M. S.; Steigerwald, M. L. *Nature* **2006**, *442*, 904.
(26) Mujica, V.; Kemp, M.; Ratner, M. A. *J. Chem. Phys.* **1994**, *101*, 6856.
(27) Joachim, C.; Ratner, M. A. *Proc. Natl. Acad. Sci. U.S.A.* **2005**, *102*, 8801.
(28) Tian, W.; Datta, S.; Hong, S.; Reifenberger, R.; Henderson, S. I.; Kubiak, C. P. *J. Chem. Phys.* **1998**, *109*, 2874.
(29) Nitzan, A. *Annu. Rev. Phys. Chem.* **2001**, *52*, 681.
(30) Tsuji, Y; Staykov, A; Yoshizawa, K. *J. Am. Chem. Soc.* **2011**, *133*, 5955.